



26

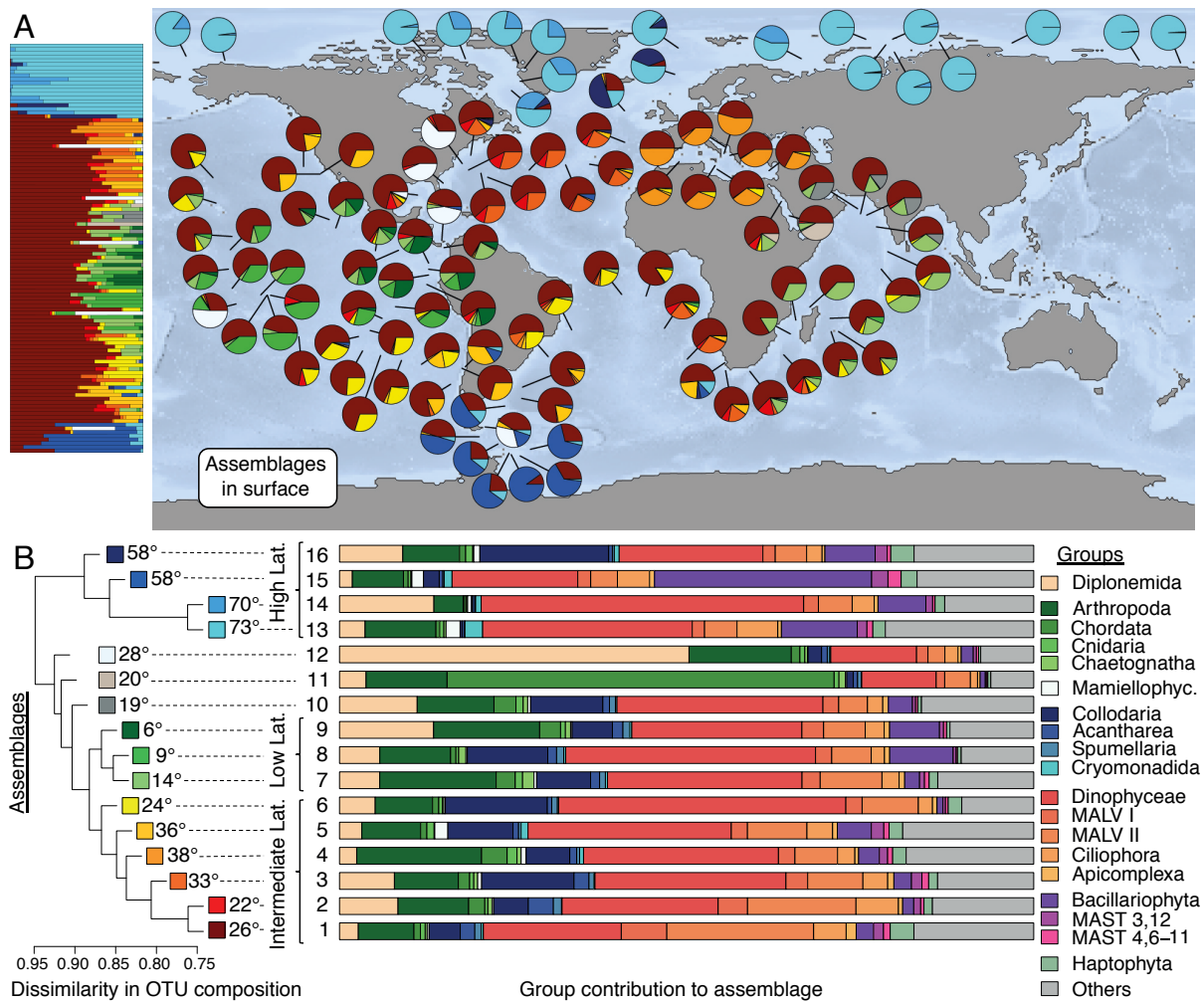
27 **Main text:** Marine plankton communities play key ecological roles at the base of oceanic  
28 food chains, and in driving global biogeochemical fluxes (1, 2). Understanding their spatial  
29 patterns of distribution is a long-standing challenge in marine ecology that has lately become  
30 a key part of the effort to model the response of oceans to environmental changes (3–6). Part  
31 of the difficulty lies in the constant recirculation of plankton communities by ocean currents,  
32 along which many physical, chemical and biological processes - the so-called *seascape* (7) -  
33 modify community composition (8). Recent planetary-scale ocean sampling expeditions have  
34 revealed that eukaryotic plankton are taxonomically and ecologically extremely diverse,  
35 possibly even more so than prokaryotic plankton (9). Eukaryotic plankton range from pico-  
36 sized (0.2-2  $\mu\text{m}$ ) to meso-sized (0.2-20 mm) organisms and larger, thus covering an  
37 exceptional range of sizes. Eukaryotic plankton also cover a wide range of ecological roles,  
38 from phototrophs (e.g., Bacillariophyta, Haptophyta, Mamiellophyceae) to parasites (e.g.,  
39 Marine Alveolates or MALVs), and from heterotrophic protists (e.g., Diplonemida,  
40 Ciliophora, Acantharea) to metazoans (e.g., Arthropoda and Chordata, respectively  
41 represented principally by Copepods and Tunicates). Understanding how these body size and  
42 ecological differences modulate the influence of oceanic currents and local environmental  
43 conditions on geographic distributions is needed if one wants to predict how eukaryotic  
44 communities, and therefore the trophic interactions and global biogeochemical cycles they  
45 participate in, will change with changing environmental conditions.

46 Previous studies suggested that all eukaryotes up to a size of approximately 1 mm are  
47 globally dispersed and primarily constrained by abiotic conditions (10). While this view has  
48 been revised, the influence of body size on biogeography is manifest (11, 12). In particular, a  
49 parallel study by Richter et al. (12), which quantified changes in plankton metagenomic  
50 composition and highlighted the underlying dynamics using transport time along main

51 currents, found that the turnover is slower, rather than faster, with increasing body size. This  
52 suggests that, rather than influencing biogeography through its effect on abundance and  
53 ultimately dispersal capacity (i.e., larger organisms are more dispersal-limited; [10](#), [11](#)), body  
54 size influences biogeography through its relationship with ecology and ultimately the  
55 sensitivity of communities to environmental conditions as they drift along currents. Under this  
56 scenario, the distribution of large long-lived generalist predators such as Copepods  
57 (Arthropoda) is expected to be stretched through large-scale transport by main currents ([8](#),  
58 [12–14](#)), and yet to be patchy as a result of small-scale turbulent stirring ([15](#)). These contrasted  
59 views illustrate that little is known on how the interplay between body size, ecology, currents  
60 and the local environment shapes biogeography ([16](#)).

61 Here, we study plankton biogeography across all major eukaryotic groups in the sunlit  
62 ocean using 18S rDNA metabarcoding data from the *Tara* Oceans global survey (including  
63 recently released data from the Arctic Ocean; [17](#)). We also used transport times from Richter  
64 et al. ([12](#)), and the same environmental data. The data encompass 250,057 eukaryotic  
65 Operational Taxonomic Units (OTUs) sampled globally at the surface and at the Deep  
66 Chlorophyll Maximum (DCM) across 129 stations. We use a probabilistic model that allows  
67 identification of a number of ‘assemblages’, each of which represents a set of OTUs that tend  
68 to co-occur across samples ([18](#), [19](#); cf. Mat. & Meth.). Each local planktonic community can  
69 then be seen as a sample drawn in various proportions from the assemblages. Across the *Tara*  
70 Oceans samples and considering all eukaryotic OTUs together, we identified 16  
71 geographically structured assemblages, each composed of OTUs covering the full taxonomic  
72 range of eukaryotic plankton (Fig. 1, S1; Appendix). Local planktonic communities often  
73 cannot be assigned to a single assemblage, as would be typical for terrestrial macro-organisms  
74 on a fixed landscape ([20](#), [21](#)), but are instead mixtures of assemblages (Fig. 1A). This is  
75 consistent with previous findings suggesting that neighbouring plankton communities are

76 continuously mixed and dispersed by currents (8, 12). Nevertheless, three assemblages are  
77 particularly represented and most communities are dominated by one of them (Fig. 1A). The  
78 most prevalent assemblage represents a set of OTUs (about one fifth of the total) that are  
79 globally ubiquitous except in the Arctic Ocean (assemblage 1, in dark red). This assemblage  
80 typically accounts for about half the number of OTUs in non-Arctic communities, and is  
81 particularly rich in parasitic groups such as MALV (Fig. 1B). The two others dominate,  
82 respectively, in the Arctic Ocean (assemblage 13, in cyan) and in the Southern Ocean  
83 (assemblage 15, in marine blue), and are particularly rich in diatoms (Fig. 1B). Based on  
84 similarity in their OTU composition, the assemblages cluster into three main categories  
85 corresponding to low, intermediate and high latitudes (Fig. 1B). The transition between  
86 communities composed of high-latitude and lower-latitude assemblages is fairly abrupt, and  
87 occurs around 45° in the North Atlantic and -47° in the South Atlantic, namely at the latitude  
88 of the subtropical front, where the transition between cold and warm waters takes place (Fig.  
89 1A&B; 22).  
90

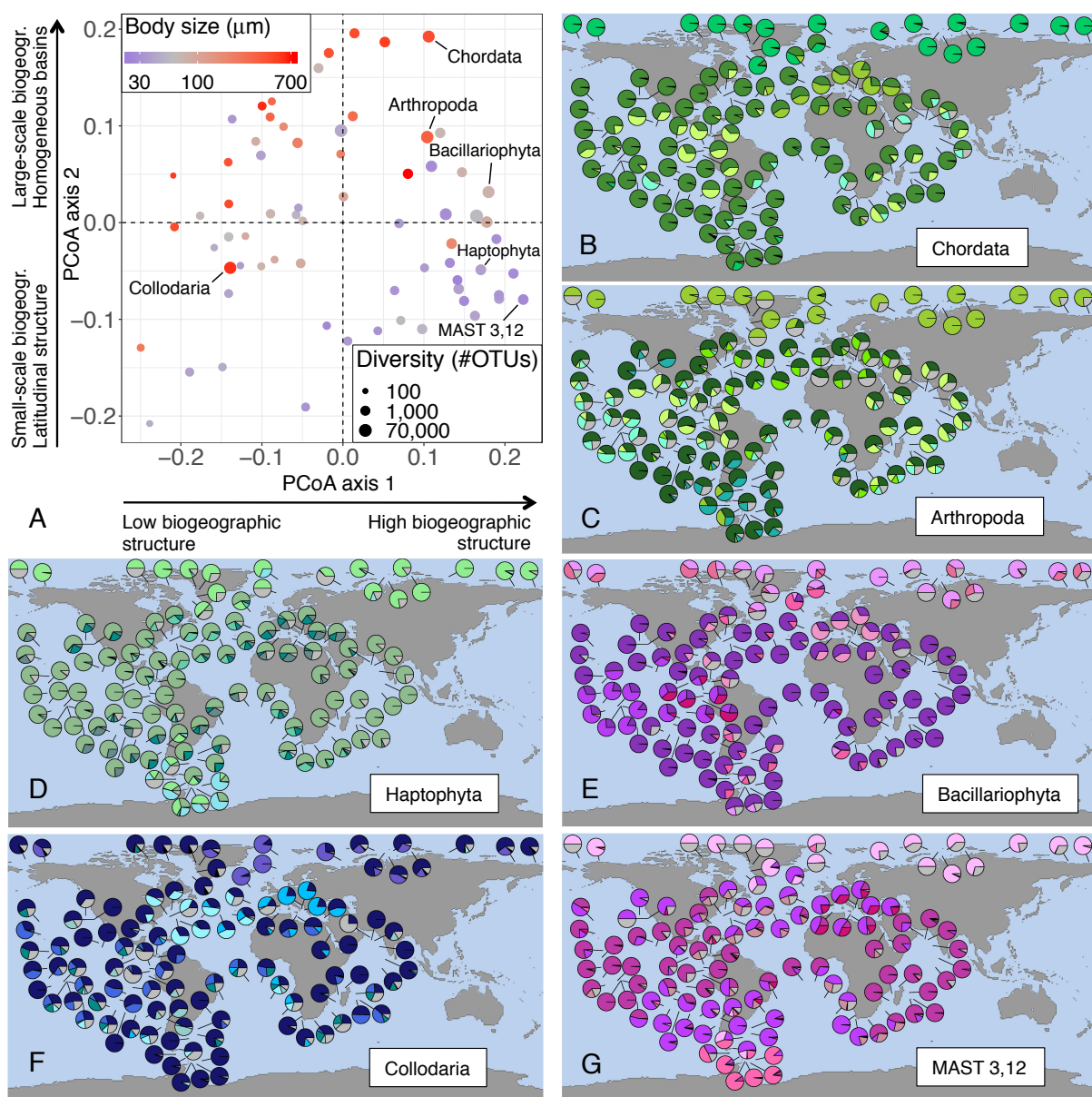


91  
 92 **Fig. 1. Global surface biogeography of eukaryotic plankton.** The biogeography of all eukaryotic  
 93 OTUs across *Tara* Oceans stations is characterized by 16 assemblages of co-occurring OTUs, each  
 94 represented by a distinct color (in A and left side of B) and identified by a number from 1 to 16 (in B).  
 95 (A) Relative contribution of the 16 assemblages to surface plankton community in *Tara* Oceans  
 96 stations, represented as pies on the world map, and as stacked bars vertically ordered by latitude on the  
 97 left-hand side of the map. (B) To the left: dendrogram of assemblage dissimilarity with respect to their  
 98 composition in OTUs (Simpson dissimilarity). The mean absolute latitude at which each assemblage is  
 99 found is indicated. Three clusters can be distinguished: a high-latitude cluster — the most distinctive  
 100 — in shades of blue, an intermediate-latitude cluster in shades from yellow to red, and a low-latitude  
 101 cluster in shades of green. To the right: barplot displaying the contribution of major eukaryotic groups  
 102 (deep-branching monophyletic groups) to assemblages. The 19 groups shown in the barplot are those  
 103 tallying more than 1,000 OTUs, grouped by phylogenetic relatedness.

104

105           This global analysis hides a strong heterogeneity across the 70 most diversified deep-  
106 branching groups of eukaryotic plankton (Table S1). Comparing the biogeography of these  
107 major groups using a normalized information-theoretic metric of dissimilarity (23; cf. Mat. &  
108 Meth.), we found high pairwise dissimilarity values (ranging between 0.64 and 0.97; Fig. S2).  
109 This heterogeneity can be decomposed into two main interpretable axes of variation (Fig. 2;  
110 cf. Mat. & Meth.). The first axis reflects the *amount* of biogeographic structure: group  
111 position on this axis is positively correlated to short-distance spatial autocorrelation  
112 (Pearson's correlation coefficient  $\rho = 0.91$  at the surface; Fig. S3A), which measures the  
113 tendency for close-by communities to be composed of the same assemblages (cf. Mat. &  
114 Meth.). Groups scoring low on this axis are characterized by strong local variation, or  
115 "patchiness". The second axis reflects the *nature* of the biogeographic structure: group  
116 position on this axis is positively correlated to the scale of biogeographic organization, which  
117 we measured as the characteristic distance at which spatial autocorrelation vanishes ( $\rho =$   
118  $0.53$ ,  $p = 10^{-6}$  at the surface; Fig. S3B) and which ranges from  $\sim 7,000$  to  $\sim 14,400$  km across  
119 groups. Group position on the second axis is also positively correlated to within-basin  
120 autocorrelation ( $\rho = 0.56$ ,  $p = 10^{-7}$  at the surface; Fig. S3C), which measures the tendency  
121 for communities from the same oceanic basin (e.g., North Atlantic, South Atlantic,  
122 Mediterranean, Southern Ocean) to be composed of the same assemblages, and negatively  
123 correlated with latitudinal autocorrelation ( $\rho = -0.49$ ,  $p = 10^{-5}$  at the surface; S3D), which  
124 measures the tendency for communities at the same latitude on both sides of the Equator to be  
125 composed of the same assemblages (cf. Mat. & Meth.). Results are similar at the DCM,  
126 although less pronounced (Fig. S4). The 70 groups of eukaryotic plankton cover the full  
127 spectra of biogeographies (Fig. 2, Fig. S5, Table S1), from those with weak spatial  
128 organization, or high patchiness (i.e., scoring low on the first axis, such as Collodaria or

129 Basidiomycota), to those organized at large spatial scale by oceanic basin (i.e., scoring high  
130 on both axes, such as Chordata or Arthropoda), and those organized at smaller spatial scale  
131 and according to latitude (i.e., scoring high on the first and low on the second axis, such as  
132 Mamiellophyceae, Haptophyta or MAST 3,12). These striking differences across planktonic  
133 groups suggest that accounting for their specificities is crucial to understanding their  
134 biogeography.  
135



137 **Fig. 2. Biogeographic heterogeneity across major eukaryotic plankton groups.** (A) Principal  
138 Coordinate Analysis (PCoA) of the biogeographic dissimilarity between 70 major groups of

139 eukaryotic plankton. Each dot corresponds to the projection of a specific plankton group onto the first  
140 two axes of variation. Position along the first axis reflects the amount of biogeographic structure  
141 displayed by the group, from a patchy distribution with weak short-distance spatial autocorrelation on  
142 the left to a structured distribution with strong short-distance spatial autocorrelation on the right.  
143 Position along the second axis reflects the nature of biogeographic structure, from a biogeography  
144 structured by latitude at the bottom to a biogeography structured by oceanic basins at the top, as well  
145 as the scale of biogeographic organization, from small to large scale. Dot size is proportional to the log  
146 diversity of the corresponding group, and dot color represents its mean log body-size, from small  
147 (blue) to large (red). **(B-G)** Surface biogeography of six major eukaryotic plankton groups. The  
148 relative contribution of the 5 to 7 most prevalent assemblages is shown in color, and that of the  
149 remaining assemblages is shown in gray; the color used for the most prevalent assemblage  
150 corresponds to the color used in Fig. 1B for the corresponding group.

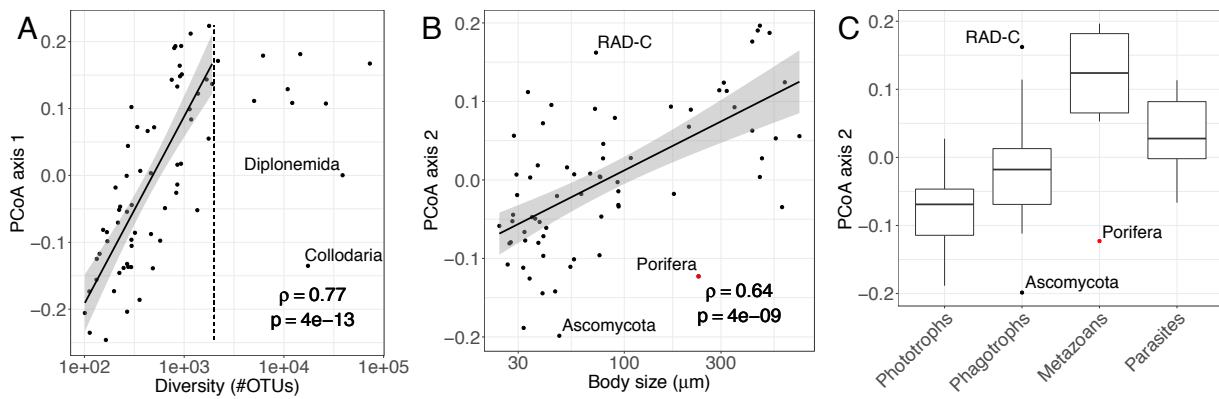
151

152 We investigated how biogeographic differences among major groups relate to their  
153 diversity, body size, and ecology, coarsely defined as either phototroph, phagotroph,  
154 metazoan or parasite (cf. Mat. & Meth.). We found that the amount of biogeographic structure  
155 (group position on the first axis) is strongly correlated to diversity ( $\rho = 0.77$ ,  $p = 10^{-13}$   
156 below 2,000 OTUs; Fig. 3A). This suggests that the maintenance of eukaryotic plankton  
157 diversity over ecological and possibly evolutionary scales is tightly linked to biogeographic  
158 structure, which may for example promote endemism. This relationship vanishes however for  
159 groups larger than about 2,000 OTUs, and two of the most diverse groups (Diplonemida,  
160 38,769 OTUs and Collodaria, 17,417 OTUs) exhibit comparatively weak biogeographic  
161 structure. The amount of biogeographic structure is weakly anticorrelated to body size  
162 ( $\rho = -0.32$ ,  $p = 0.007$ ; Fig. S6A), and after accounting for differences in diversity across  
163 groups, is lower for metazoans than for phototrophs (ANCOVA t-test:  $p = 0.04$ , Fig. S6B), in  
164 agreement with the expectation of a higher local patchiness in their distribution induced by



165 turbulent stirring (15, 24). In contrast, the nature of biogeographic structure (group position  
166 on the second axis) is strongly correlated to body size ( $\rho = 0.64$ ,  $p = 10^{-9}$ ; Fig. 3B) and  
167 ecology (ANOVA F-test:  $p = 10^{-7}$ , Fig. 3C), and only weakly to diversity ( $\rho = 0.24$ ,  
168  $p = 0.05$ ; Fig. S6C). Metazoan groups score high on the second axis of variation (with the  
169 notable exception of Porifera sponges, probably at the larval stage, which are excluded from  
170 statistical results) and phototrophs score low, while phagotrophs occupy an intermediate  
171 position, spanning a comparatively wider range of biogeographies (Fig. 3C). Parasites are just  
172 below metazoans, which suggests that their biogeography is influenced by that of their hosts.  
173 While body size covaries with ecology (phagotrophs are larger than phototrophs on average,  
174 and metazoans significantly larger than other plankton types; Fig. S7), the positive  
175 relationship between group position on the second axis and body size still holds within each  
176 of the four ecological categories (ANCOVA F-test:  $p = 10^{-4}$ ; Fig. S8). Diatoms  
177 (Bacillariophyta) are a striking example: of all phototrophs, they have the largest body size  
178 and also score highest on the second axis of variation. Conversely, ecology significantly  
179 influences group position on the second axis even after accounting for body size differences  
180 (ANCOVA F-test:  $p = 0.01$ ). Collodaria, which we did not assign to an ecological category,  
181 score lower than expected from their large body size, but close to the average for  
182 phagotrophic groups (Fig. 2, Table S1). These results suggest that biogeographic patterns are  
183 influenced by both body size and ecology. To summarize, diversity-rich groups are  
184 biogeographically structured, with large-bodied heterotrophs (metazoans such as Copepods  
185 and Tunicates) exhibiting biogeographic variations at the scale of oceanic basins or larger,  
186 and small-bodied phototrophs (such as Haptophyta) at smaller spatial scale and following  
187 latitude (Fig. 2).

188



189

190 **Fig. 3. Relationship between biogeography and diversity, mean body size and ecology across**  
191 **major eukaryotic plankton groups.** (A) The position of the 70 plankton groups along the first axis of  
192 biogeographic variation, indicative of the amount of biogeographic structure, increases sharply with  
193 log diversity (number of OTUs in the group) up to approximately 2,000 OTUs, but not beyond (as  
194 exemplified by Diplonemida and Collodaria, two of the most diverse groups). (B) The position of the  
195 70 plankton groups along the second axis, indicative of the nature and spatial scale of biogeographic  
196 structure, increases with log mean body size, indicating that large-bodied plankton is organized at  
197 larger spatial scale and according to oceanic basins rather than latitude. (C) Positions along the second  
198 axis of plankton groups binned into four broad ecological categories (Collodaria and Dynophyceae  
199 were not categorized and are therefore not represented). Pairwise differences are all significant except  
200 between Phagotrophs and Parasites. The grey dot denotes Porifera, an outlier group excluded from  
201 statistical tests.

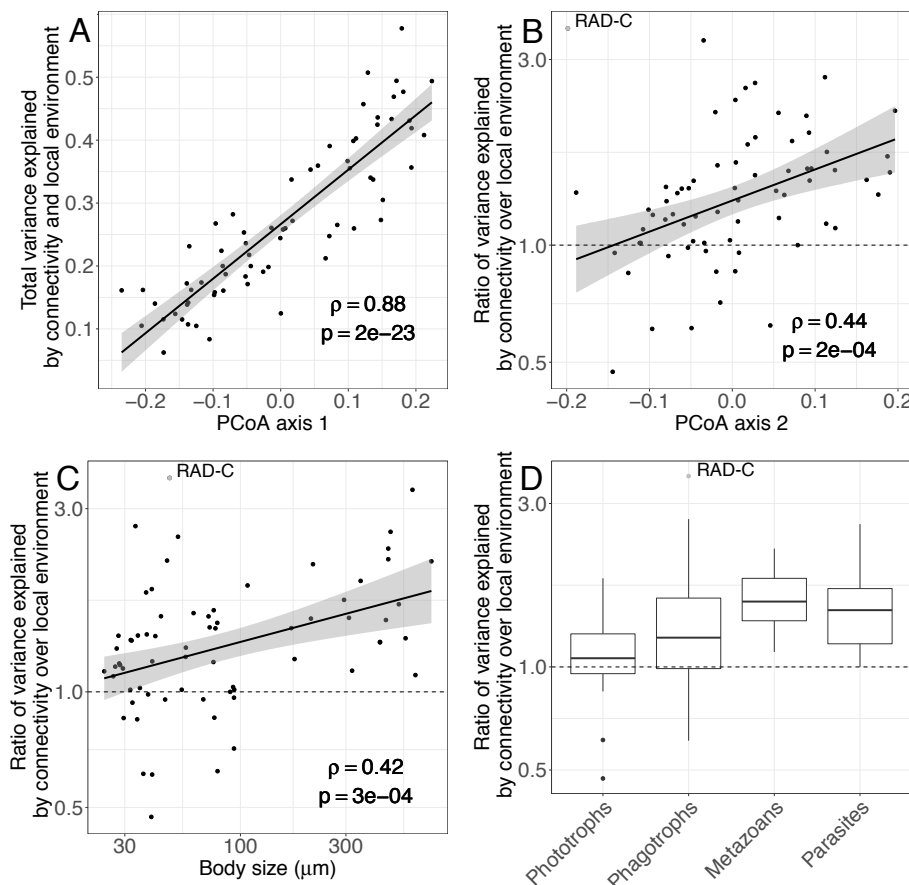
202

203 A global biogeography matching oceanic basins suggests that communities respond to  
204 environmental variations slowly enough to be homogenised by ocean circulation at the basin  
205 scale (i.e., gyres; [12](#)), but have little ability to disperse between basins, either due to the  
206 comparatively limited connectivity by currents or to environmental barriers, and therefore that  
207 their biogeography is primarily shaped by the main ocean currents ([13](#)). Conversely, a  
208 biogeography matching latitude, symmetric with respect to the Equator, suggests a faster  
209 response of communities to environmental variations within basins (which are structured by  
210 latitude and currents, e.g. the cross-latitude influence of the Gulf Stream), low cross-basin

211 dispersal limitation, and therefore a comparatively more important role of local environmental  
212 filtering in shaping biogeography. To explain the global biogeography of major taxonomic  
213 groups, we compared biogeographic maps to maps of connectivity by currents and  
214 environmental conditions. We transformed the matrix of minimum transport times between  
215 pairs of stations, previously computed from a global ocean circulation model ([12](#), [25](#)), into  
216 spatial patterns at different scales through eigenvector decomposition, thus obtaining a set of  
217 so-called Moran Eigenvector maps (thereafter simply referred to as “connectivity maps”; cf.  
218 Mat. & Meth.). These maps represent the hypothetical geographic patterns expected for  
219 plankton with temporal variation along currents matching these scales (Fig. S9, S10). We  
220 estimated local abiotic conditions using yearly-averaged measurements of temperature,  
221 nutrient concentration and oxygen availability (World Ocean Atlas 2013; [26](#); cf. Mat. &  
222 Meth.). Because biotic interactions (predation, competition, parasitic and mutualistic  
223 symbiosis) are thought to be important determinants of plankton community structure ([27](#)),  
224 we also quantified local biotic conditions using the relative read counts of major eukaryotic  
225 groups (excluding the focal group; cf. Mat. & Meth.). Biotic conditions, similarly to abiotic  
226 ones, have a latitudinal structure, and we refer here to them collectively as ‘environmental  
227 conditions’ (Fig. S11, S12). The resulting environmental maps can be interpreted as the  
228 hypothetical geographic patterns expected for organisms with a fast response to local  
229 environmental conditions and whose dispersal by currents is not limiting. Hence, a  
230 biogeography matching connectivity maps better than environmental maps suggest that the  
231 constraints imposed by the seascape, that is the transport of plankton by oceanic currents  
232 modulated by mixing and ecological drift, but also by the responses to nutrient supplies and  
233 temperature variations during transport, dominate over those imposed by detectable local  
234 environmental filtering (see also [12](#)).

235 We found that the total variance in surface community composition that can be  
236 explained by connectivity maps and local environmental conditions (abiotic and biotic)  
237 averages 27% across groups (min. 0% for Porifera, max. 58%) and is, as expected, tightly  
238 correlated to the amount of biogeographic structure ( $\rho = 0.88$ ; Fig. 4A; cf. Mat. & Meth.).  
239 The part of the variance that is statistically explained by connectivity patterns is primarily  
240 contributed by between-basin connectivity patterns (Fig. S10 & S13), and is for most groups  
241 larger than the part of the variance statistically explained by environmental data (at the  
242 surface, on average 40% of the explained variance is purely explained by connectivity versus  
243 22% by the environment; Fig. S14A). This supports a prominent role of transport by the main  
244 current systems and of the processes occurring along those pathways in shaping eukaryotic  
245 plankton biogeography, both by extending the distribution of some taxa beyond their optimal  
246 range (28) and by constraining long-distance dispersal. Unmeasured environmental variations  
247 along currents likely contribute to this role of ocean circulation. As expected from our  
248 previous results, the ratio of the fractions of variance explained by connectivity patterns and  
249 environmental data, which reflects their relative contributions to biogeography, increases with  
250 group position on the second axis of variation ( $\rho = 0.44$ ,  $p = 10^{-4}$ ; Fig. 4B). Accordingly,  
251 the relative contribution of connectivity by currents also increases with average group body  
252 size ( $\rho = 0.42$ ,  $p = 10^{-4}$ ; Fig. 4C) and depends on ecology (ANOVA F-test:  $p = 0.003$ ; Fig.  
253 4D). These results indicate that metazoans are closer to drifting tracers strongly influenced by  
254 currents, and constrained in particular by limited between-basin connectivity, while  
255 phototrophs are more strongly coupled with environmental factors and disperse more readily  
256 between basins. The difference in sensitivity to local environmental conditions can be  
257 explained by differences in ecological requirements and community dynamics. Why there is a  
258 difference in between-basins dispersal is less clear. All basins are connected by currents  
259 within a few years of transport time (29), and small phototrophs may have a higher ability to

260 disperse through environmental barriers by forming spores or dormant states (10).  
261 Alternatively, the looser environmental coupling and slower dynamics of metazoan  
262 communities might make them more sensitive to the smaller between-basin compared to  
263 within-basin water flow. Finally, within the variance explained by the local environment, an  
264 approximately equal share can be attributed to biotic and abiotic conditions for most groups  
265 (respectively 29% and 26% purely explained at the surface, on average; Fig. S14B),  
266 irrespective of their body size, ecology, diversity or biogeography (Fig. S15). Results are  
267 similar at the DCM, but are far less pronounced (Fig. S16, S17). Although we cannot exclude  
268 the possibility that local biotic conditions reflect the indirect effect of local abiotic factors that  
269 are not accounted for in our study, such as fluxes of nutrients, which are often more relevant  
270 to planktonic organisms than instantaneous nutrient concentrations (28), these results indicate  
271 an additional role for interspecific interactions in shaping community composition (27, 30).  
272



273

274 **Fig. 4. Drivers of surface biogeography across major eukaryotic plankton groups.** (A) The total  
275 variance in surface biogeography that can be explained by the combination of connectivity by currents  
276 and (abiotic and biotic) local environmental conditions increases with the position of plankton groups  
277 on the first axis of biogeographic variation. (B-D) Across major plankton groups, the log ratio of the  
278 variance explained by connectivity over the variance explained by (abiotic and biotic) local  
279 environmental conditions (B) increases with group position on the second axis of variation, (C)  
280 increases with log mean body size, and (D) varies across broad ecological categories (pairwise  
281 differences are significant except Metazoans-Parasites and Phagotrophs-Phototrophs). The ratio is  
282 higher than 1 for most groups, reflecting an overall stronger influence of connectivity by currents  
283 compared to local environmental conditions on plankton biogeography at the surface. The grey dot  
284 denotes RAD-C, an outlier group excluded from statistical tests. We did not find any significant  
285 explanatory variable for Porifera and therefore excluded this group from these analyses.

286

287 Our study clarifies the patterns and processes underlying the global biogeography of  
288 the main groups of eukaryotic plankton in the sunlit ocean. Consistent with metagenomic  
289 results at lower taxonomic resolution (12), we find that eukaryotic plankton exhibits a global-  
290 scale biogeography, and that community variation is slow enough along currents to allow  
291 them to be the dominant driver of this biogeography. The continuous movement of water  
292 masses generates biogeographic patterns that are better represented by overlapping taxa  
293 assemblages than by the well-delineated biomes characteristic of terrestrial systems. Our  
294 comparison of eukaryotic plankton groups reveals several additional results. First, the  
295 geographic structuring induced by currents may have favored the generation and maintenance  
296 of eukaryotic plankton diversity. Second, plankton ecology matters beyond body size  
297 differences, and reciprocally body size matters beyond ecological differences. Third, body  
298 size and ecology influence primarily the nature of biogeographic patterns, namely their spatial  
299 scale of organization and whether they are organized by oceanic basins or latitude, and only

300 secondarily the amount of biogeographic structure, namely local patchiness. Fourth, biotic  
301 conditions appear to be at least as important a driver of biogeography as local abiotic  
302 conditions. Our results reconcile the views that larger-bodied organisms are more dispersal-  
303 limited (*10, 11*) and yet display a slower compositional turnover along currents than smaller  
304 organisms (*12*): at the global scale, organisms of larger sizes are indeed more dispersal-  
305 limited; however at the regional scale, they have wider spatial distributions, presumably  
306 linked to their specific ecologies, longer lifespan and reduced sensitivity to local  
307 environmental variations. At the two extremes, metazoan heterotrophs are structured at the  
308 scale of oceanic basins following the main currents, while small phototrophs are structured  
309 latitudinally with a comparatively larger influence of local environmental conditions,  
310 including biotic ones. Together, our results suggest that predictive modeling of plankton  
311 communities in a changing environment (*17, 31*) will critically depend on our ability to model  
312 the impact of changes in ocean currents and to develop niche models accounting for both  
313 species ecology and interspecific interactions.

314 **References and Notes**

315

316 1. C. B. Field, M. J. Behrenfeld, J. T. Randerson, P. Falkowski, Primary production of  
317 the biosphere: integrating terrestrial and oceanic components. *Science*. **281**, 237–240  
318 (1998).

319 2. A. Z. Worden, M. J. Follows, S. J. Giovannoni, S. Wilken, A. E. Zimmerman, P. J.  
320 Keeling, Rethinking the marine carbon cycle: Factoring in the multifarious lifestyles  
321 of microbes. *Science*. **347**, 1257594 (2015).

322 3. G. Beaugrand, R. R. Kirby, How Do Marine Pelagic Species Respond to Climate  
323 Change? Theories and Observations. *Annual Review of Marine Science*. **10**, 169–197  
324 (2018).

325 4. E. J. Raes, L. Bodrossy, J. van de Kamp, A. Bissett, M. Ostrowski, M. V. Brown, S. L.  
326 S. Sow, B. Sloyan, A. M. Waite, Oceanographic boundaries constrain microbial  
327 diversity gradients in the South Pacific Ocean. *Proceedings of the National Academy  
328 of Sciences*. **115**, E8266–E8275 (2018).

329 5. D. Righetti, M. Vogt, N. Gruber, A. Psomas, N. E. Zimmermann, Global pattern of  
330 phytoplankton diversity driven by temperature and environmental variability. *Science  
331 Advances*. **5**, eaau6253 (2019).

332 6. D. P. Tittensor, C. Mora, W. Jetz, H. K. Lotze, D. Ricard, E. V. Berghe, B. Worm,  
333 Global patterns and predictors of marine biodiversity across taxa. *Nature*. **466**, 1098–  
334 1101 (2010).

335 7. M. T. Kavanaugh, M. J. Oliver, F. P. Chavez, R. M. Letelier, F. E. Muller-Karger, S.  
336 C. Doney, Seascapes as a new vernacular for pelagic ocean monitoring, management  
337 and conservation. *ICES J Mar Sci*. **73**, 1839–1850 (2016).

338 8. M. Lévy, O. Jahn, S. Dutkiewicz, M. J. Follows, Phytoplankton diversity and



- 339 community structure affected by oceanic dispersal and mesoscale turbulence. *Limnol.*  
340 *Oceanogr.* **4**, 67–84 (2014).
- 341 9. C. de Vargas, S. Audic, N. Henry, J. Decelle, F. Mahe, R. Logares, E. Lara, C.  
342 Berney, N. Le Bescot, I. Probert, M. Carmichael, J. Poulain, S. Romac, S. Colin, J.-M.  
343 Aury, L. Bittner, S. Chaffron, M. Dunthorn, S. Engelen, O. Flegontova, L. Guidi, A.  
344 Horak, O. Jaillon, G. Lima-Mendez, J. Lukes, S. Malviya, R. Morard, M. Mulot, E.  
345 Scalco, R. Siano, F. Vincent, A. Zingone, C. Dimier, M. Picheral, S. Searson, S.  
346 Kandels-Lewis, S. G. Acinas, P. Bork, C. Bowler, G. Gorsky, N. Grimsley, P.  
347 Hingamp, D. Iudicone, F. Not, H. Ogata, S. Pesant, J. Raes, M. E. Sieracki, S. Speich,  
348 L. Stemmann, S. Sunagawa, J. Weissenbach, P. Wincker, E. Karsenti, C. Tara Oceans,  
349 Eukaryotic plankton diversity in the sunlit ocean. *Science*. **348**, 1261605 (2015).
- 350 10. B. J. Finlay, Global Dispersal of Free-Living Microbial Eukaryote Species. *Science*.  
351 **296**, 1061–1063 (2002).
- 352 11. E. Villarino, J. R. Watson, B. Jönsson, J. M. Gasol, G. Salazar, S. G. Acinas, M.  
353 Estrada, R. Massana, R. Logares, C. R. Giner, M. C. Pernice, M. P. Olivar, L. Citores,  
354 J. Corell, N. Rodríguez-Ezpeleta, J. L. Acuña, A. Molina-Ramírez, J. I. González-  
355 Gordillo, A. Cózar, E. Martí, J. A. Cuesta, S. Agustí, E. Fraile-Nuez, C. M. Duarte, X.  
356 Irigoien, G. Chust, Large-scale ocean connectivity and planktonic body size. *Nature*  
357 *Communications*. **9**, 142 (2018).
- 358 12. D. J. Richter, R. Watteaux, T. Vannier, J. Leconte, P. Frémont, G. Reygondeau, N.  
359 Maillet, N. Henry, G. Benoit, A. Fernández-Guerra, S. Suweis, R. Narci, C. Berney,  
360 D. Eveillard, F. Gavory, L. Guidi, K. Labadie, E. Mahieu, J. Poulain, S. Romac, S.  
361 Roux, C. Dimier, S. Kandels, M. Picheral, S. Searson, T. O. Coordinators, S. Pesant,  
362 J.-M. Aury, J. R. Brum, C. Lemaitre, E. Pelletier, P. Bork, S. Sunagawa, L. Karp-  
363 Boss, C. Bowler, M. B. Sullivan, E. Karsenti, M. Mariadassou, I. Probert, P.

- 364 Peterlongo, P. Wincker, C. de Vargas, M. R. d'Alcalà, D. Iudicone, O. Jaillon, T. O.  
365 Coordinators, Genomic evidence for global ocean plankton biogeography shaped by  
366 large-scale current systems. *bioRxiv*, 867739 (2019).
- 367 13. F. L. Hellweger, E. van Sebille, N. D. Fredrick, Biogeographic patterns in ocean  
368 microbes emerge in a neutral agent-based model. *Science*. **345**, 1346–1349 (2014).
- 369 14. M.-A. Madoui, J. Poulain, K. Sugier, M. Wessner, B. Noel, L. Berline, K. Labadie, A.  
370 Cornils, L. Blanco-Bercial, L. Stemmann, J.-L. Jamet, P. Wincker, New insights into  
371 global biogeography, population structure and natural selection from the genome of  
372 the epipelagic copepod *Oithona*. *Molecular Ecology*. **26**, 4467–4482 (2017).
- 373 15. E. R. Abraham, The generation of plankton patchiness by turbulent stirring. *Nature*.  
374 **391**, 577–580 (1998).
- 375 16. L. Oziel, A. Baudena, M. Ardyna, P. Massicotte, A. Randelhoff, J.-B. Sallée, R. B.  
376 Ingvaldsen, E. Devred, M. Babin, Faster Atlantic currents drive poleward expansion of  
377 temperate phytoplankton in the Arctic Ocean. *Nat Commun*. **11**, 1–8 (2020).
- 378 17. F. M. Ibarbalz, N. Henry, M. C. Brandão, S. Martini, G. Busseni, H. Byrne, L. P.  
379 Coelho, H. Endo, J. M. Gasol, A. C. Gregory, F. Mahé, J. Rigonato, M. Royo-Llonch,  
380 G. Salazar, I. Sanz-Sáez, E. Scalco, D. Soviadan, A. A. Zayed, A. Zingone, K.  
381 Labadie, J. Ferland, C. Marec, S. Kandels, M. Picheral, C. Dimier, J. Poulain, S.  
382 Pisarev, M. Carmichael, S. Pesant, S. G. Acinas, M. Babin, P. Bork, E. Boss, C.  
383 Bowler, G. Cochrane, C. de Vargas, M. Follows, G. Gorsky, N. Grimsley, L. Guidi, P.  
384 Hingamp, D. Iudicone, O. Jaillon, S. Kandels, L. Karp-Boss, E. Karsenti, F. Not, H.  
385 Ogata, S. Pesant, N. Poulton, J. Raes, C. Sardet, S. Speich, L. Stemmann, M. B.  
386 Sullivan, S. Sunagawa, P. Wincker, M. Babin, E. Boss, D. Iudicone, O. Jaillon, S. G.  
387 Acinas, H. Ogata, E. Pelletier, L. Stemmann, M. B. Sullivan, S. Sunagawa, L. Bopp,  
388 C. de Vargas, L. Karp-Boss, P. Wincker, F. Lombard, C. Bowler, L. Zinger, Global

- 389 Trends in Marine Plankton Diversity across Kingdoms of Life. *Cell*. **179**, 1084-  
390 1097.e21 (2019).
- 391 18. G. Sommeria-Klein, L. Zinger, E. Coissac, A. Iribar, H. Schimann, P. Taberlet, J.  
392 Chave, Latent Dirichlet Allocation reveals spatial and taxonomic structure in a DNA-  
393 based census of soil biodiversity from a tropical forest. *Molecular Ecology Resources*.  
394 **20**, 371–386 (2019).
- 395 19. D. Valle, B. Baiser, C. W. Woodall, R. Chazdon, Decomposing biodiversity data using  
396 the Latent Dirichlet Allocation model, a probabilistic multivariate statistical method.  
397 *Ecology Letters*. **17**, 1591–1601 (2014).
- 398 20. A. R. Wallace, *The geographical distribution of animals: with a study of the relations*  
399 *of living and extinct faunas as elucidating the past changes of the earth's surface*  
400 (Cambridge University Press, 1876), vol. 1.
- 401 21. G. F. Ficetola, F. Mazel, W. Thuiller, Global determinants of zoogeographical  
402 boundaries. *Nature Ecology and Evolution*. **1**, 1–7 (2017).
- 403 22. L. D. Talley, *Descriptive physical oceanography: an introduction* (Academic press,  
404 2011).
- 405 23. M. Meila, Comparing clusterings—an information based distance. *Journal of*  
406 *Multivariate Analysis*. **98**, 873–895 (2006).
- 407 24. A. Bertrand, D. Grados, F. Colas, S. Bertrand, X. Capet, A. Chaigneau, G. Vargas, A.  
408 Mousseigne, R. Fablet, Broad impacts of fine-scale dynamics on seascape structure  
409 from zooplankton to seabirds. *Nat Commun*. **5**, 1–9 (2014).
- 410 25. S. Clayton, S. Dutkiewicz, O. Jahn, C. Hill, P. Heimbach, M. J. Follows,  
411 Biogeochemical versus ecological consequences of modeled ocean physics.  
412 *Biogeosciences*. **14**, 2877–2889 (2017).
- 413 26. T. P. Boyer, J. I. Antonov, O. K. Baranova, C. Coleman, H. E. Garcia, A. Grodsky, D.

- 414 R. Johnson, R. A. Locarnini, A. V. Mishonov, T. D. O'Brien, World Ocean Database  
415 2013. (2013), doi:10.7289/V5NZ85MT.
- 416 27. G. Lima-Mendez, K. Faust, N. Henry, J. Decelle, S. Colin, F. Carcillo, S. Chaffron, J.  
417 C. Ignacio-Espinosa, S. Roux, F. Vincent, L. Bittner, Y. Darzi, J. Wang, S. Audic, L.  
418 Berline, G. Bontempi, A. M. Cabello, L. Coppola, F. M. Cornejo-Castillo, F.  
419 d'Ovidio, L. De Meester, I. Ferrera, M. J. Garet-Delmas, L. Guidi, E. Lara, S. Pesant,  
420 M. Royo-Llonch, G. Salazar, P. Sanchez, M. Sebastian, C. Souffreau, C. Dimier, M.  
421 Picheral, S. Searson, S. Kandels-Lewis, G. Gorsky, F. Not, H. Ogata, S. Speich, L.  
422 Stemmann, J. Weissenbach, P. Wincker, S. G. Acinas, S. Sunagawa, P. Bork, M. B.  
423 Sullivan, E. Karsenti, C. Bowler, C. de Vargas, J. Raes, C. Tara Oceans, Determinants  
424 of community structure in the global plankton interactome. *Science*. **348**, 1262073  
425 (2015).
- 426 28. S. Dutkiewicz, P. Cermeno, O. Jahn, M. J. Follows, A. E. Hickman, D. A. A.  
427 Taniguchi, B. A. Ward, Dimensions of marine phytoplankton diversity.  
428 *Biogeosciences*. **17**, 609–634 (2020).
- 429 29. B. F. Jönsson, J. R. Watson, The timescales of global surface-ocean connectivity.  
430 *Nature Communications*. **7**, 11239 (2016).
- 431 30. F. Vincent, C. Bowler, Diatoms Are Selective Segregators in Global Ocean Planktonic  
432 Communities. *mSystems*. **5** (2020), doi:10.1128/mSystems.00444-19.
- 433 31. H. K. Lotze, D. P. Tittensor, A. Bryndum-Buchholz, T. D. Eddy, W. W. L. Cheung, E.  
434 D. Galbraith, M. Barange, N. Barrier, D. Bianchi, J. L. Blanchard, L. Bopp, M.  
435 Büchner, C. M. Bulman, D. A. Carozza, V. Christensen, M. Coll, J. P. Dunne, E. A.  
436 Fulton, S. Jennings, M. C. Jones, S. Mackinson, O. Maury, S. Niiranen, R. Oliveros-  
437 Ramos, T. Roy, J. A. Fernandes, J. Schewe, Y.-J. Shin, T. A. M. Silva, J. Steenbeek,  
438 C. A. Stock, P. Verley, J. Volkholz, N. D. Walker, B. Worm, Global ensemble

- 439 projections reveal trophic amplification of ocean biomass declines with climate  
440 change. *Proc. Natl. Acad. Sci. U.S.A.* **116**, 12907–12912 (2019).
- 441 32. F. Mahé, T. Rognes, C. Quince, C. de Vargas, M. Dunthorn, Swarm: robust and fast  
442 clustering method for amplicon-based studies. *PeerJ*. **2**, e593 (2014).
- 443 33. L. Guillou, D. Bachar, S. Audic, D. Bass, C. Berney, L. Bittner, C. Boutte, G.  
444 Burgaud, C. de Vargas, J. Decelle, J. del Campo, J. R. Dolan, M. Dunthorn, B.  
445 Edvardsen, M. Holzmann, W. H. C. F. Kooistra, E. Lara, N. Le Bescot, R. Logares, F.  
446 Mahé, R. Massana, M. Montresor, R. Morard, F. Not, J. Pawlowski, I. Probert, A.-L.  
447 Sauvadet, R. Siano, T. Stoeck, D. Vaultot, P. Zimmermann, R. Christen, The Protist  
448 Ribosomal Reference database (PR2): a catalog of unicellular eukaryote Small Sub-  
449 Unit rRNA sequences with curated taxonomy. *Nucleic Acids Res.* **41**, D597–D604  
450 (2013).
- 451 34. D. M. Blei, A. Y. Ng, M. I. Jordan, Latent Dirichlet Allocation. *Journal of Machine*  
452 *Learning Research*. **3**, 993–1022 (2003).
- 453 35. X.-H. Phan, L.-M. Nguyen, S. Horiguchi, in *Proceeding of the 17th international*  
454 *conference on World Wide Web - WWW '08* (ACM Press, Beijing, China, 2008;  
455 <http://portal.acm.org/citation.cfm?doid=1367497.1367510>), p. 91.
- 456 36. B. Grün, K. Hornik, topicmodels: an R package for fitting topic models. *Journal of*  
457 *statistical software*. **40**, 1–30 (2011).
- 458 37. R Core Team, *R: A Language and Environment for Statistical Computing* (R  
459 Foundation for Statistical Computing, Vienna, Austria, 2018).
- 460 38. E. Paradis, K. Schliep, ape 5.0: an environment for modern phylogenetics and  
461 evolutionary analyses in R. *Bioinformatics*. **35**, 526–528 (2019).
- 462 39. P. Legendre, L. Legendre, *Numerical Ecology* (Elsevier, 2012).
- 463 40. D. Menemenlis, J.-M. Campin, P. Heimbach, C. Hill, T. Lee, M. Schodlok, H. Zhang,

- 464 ECCO2: High Resolution Global Ocean and Sea Ice Data Synthesis. *Mercator Ocean*  
465 *Quarterly Newsletter*. **31**, 13–21 (2008).
- 466 41. D. Chessel, A. Dufour, J. Thioulouse, The ade4 Package - I: One-Table Methods. *R*  
467 *News*, 5–10 (2004).
- 468 42. J. R. Watson, C. G. Hays, P. T. Raimondi, S. Mitarai, C. Dong, J. C. McWilliams, C.  
469 A. Blanchette, J. E. Caselle, D. A. Siegel, Currents connecting communities: nearshore  
470 community similarity and ocean circulation. *Ecology*. **92**, 1193–1200 (2011).
- 471 43. D. Wilkins, E. van Sebille, S. R. Rintoul, F. M. Lauro, R. Cavicchioli, Advection  
472 shapes Southern Ocean microbial assemblages independent of distance and  
473 environment effects. *Nature Communications*. **4**, 1–7 (2013).
- 474 44. J. Oksanen, F. G. Blanchet, M. Friendly, R. Kindt, P. Legendre, D. McGlinn, P. R.  
475 Minchin, R. B. O’Hara, G. L. Simpson, P. Solymos, M. H. H. Stevens, E. Szoecs, H.  
476 Wagner, *vegan: Community Ecology Package* (2018).
- 477 45. Clayton Sophie, Dutkiewicz Stephanie, Jahn Oliver, Follows Michael J., Dispersal,  
478 eddies, and the diversity of marine phytoplankton. *Limnology and Oceanography:*  
479 *Fluids and Environments*. **3**, 182–197 (2012).
- 480 46. S. Dutkiewicz, P. Cermeno, O. Jahn, M. J. Follows, A. E. Hickman, D. A. A.  
481 Taniguchi, B. A. Ward, Dimensions of Marine Phytoplankton Diversity.  
482 *Biogeosciences Discussions*, 1–46 (2019).
- 483 47. J. Hausser, K. Strimmer, *entropy: estimation of entropy, mutual information and*  
484 *related quantities* (2014).

485

486 **Acknowledgements**

487

488 We are grateful to Federico Ibarbalz for his essential help with the data. We thank Olivier  
489 Jaillon and Colomban de Vargas for feedback and early discussions on the project. We thank  
490 Mick Follows and Oliver Jahn for sharing MITgcm simulation results for the Arctic Ocean.  
491 We thank Florian Hartig and Odile Maliet for their guidance on Bayesian inference, Leandro  
492 Arístide and Felipe Delestro for their kind assistance with the figures, and Carmelo Fruciano  
493 and Benoît Perez for their advice on statistics. We thank Fabio Benedetti, Julien Clavel, Elena  
494 Kazamia, Sophia Lambert, Eric Lewitus, Marc Manceau, Olivier Missa, Silvia de Monte,  
495 Isaac Overcast, Ignacio Quintero, Enrico Ser-Giacomi, Ana Catarina Silva and Flora Vincent  
496 for suggestions and fruitful discussions.

497

498 **Funding:** This work was supported by *European Research Council* grants (ERC 616419-  
499 PANDA, to H.M.; ERC 835067-DIATOMIC, to C.B.), grants from the French *Agence*  
500 *Nationale de la Recherche* (MEMOLIFE, ref. ANR-10-LABX-54, to G.S.K., H.M. and C.B.;  
501 OCEANOMICS, ref. ANR-11-BTBR-0008, to C.B.) and funds from CNRS. C.B. and H.M.  
502 are members of the Research Federation for the study of Global Ocean Systems Ecology and  
503 Evolution, FR2022/Tara Oceans GOSEE. This article is contribution number XXX of *Tara*  
504 Oceans.

505

506 **Author contributions:** GSK and HM designed the study with the help of RW, DI and CB.  
507 GSK performed the analyses. RW contributed the transport time data and their interpretation.  
508 GSK and HM wrote the paper with substantial input from RW, DI and CB.

509

510 **Competing interests:** The authors declare no competing financial interests.

511

512 **Data availability:** All data reported herein are available without restrictions. Metabarcoding  
513 data have been deposited at the European Nucleotide Archive (ENA) under accession  
514 numbers PRJEB6610 and PRJEB9737. Sample metadata are available from  
515 <https://doi.org/10.1594/PANGAEA.875582>.



516 **List of Supplementary Material**

517

518 Materials and Methods

519 Appendix

520 Figures S1 to S17

521 Table S1

522 References (32-47)